CHAPTER 1

The Cartesian Method of Profile Migration

Profile migration consists of the downward continuation of an upgoing wavefield recorded by the geophones, the downward continuation of a downgoing wavefield caused by a shot, and imaging. The Cartesian method for migrating profiles performs these three operations in an orthonormal coordinate system with axes for time, depth, and lateral position. After migration, the profile images can be stacked to suppress noise. Formal discussions of the operations performed by a Cartesian profile migration algorithm are found in the first three sections of this chapter. The fourth section consists of a more detailed description of the organization of a Cartesian profile migration algorithm that downward continues both upgoing and downgoing waves computationally.

Downward continuation of the upgoing wave

Downward continuation of the wavefield U, recorded by the geophones of a profile, is performed with a one-way acoustic wave equation. The justification for this procedure involves the approximation of the wavefield recorded by the geophones as consisting entirely of upwards traveling acoustic waves obeying a one-way acoustic wave equation. This wave equation is enough as along as multiples are not overpowering.

A one-way wave equation for downward continuing upwards traveling acoustic waves can be derived from the full two-way acoustic wave equation. Consider the two-way wave equation for a pressure deviation wavefield $U(x,z,t)$ traveling through a medium with constant acoustic velocity v.

$$\frac{\partial^2 U}{\partial z^2} = \frac{1}{v^2}\frac{\partial^2 U}{\partial t^2} - \frac{\partial^2 U}{\partial x^2} \tag{1}$$

where x is the lateral position of the receiver recording the pressure wave field at the surface. If the wave field at the surface is independent of x, so that $U(x,0,t) = f(t)$, then the wave field in the subsurface must be the sum of a function of $z - vt$, a downgoing wave, with a function of $z + vt$, an upgoing wave. A first order differential equation in z that propagates only upgoing waves is

$$\frac{\partial}{\partial z} U = \frac{1}{v}\frac{\partial}{\partial t} U \approx \left[\frac{1}{v^2}\frac{\partial^2}{\partial t^2}\right]^{1/2} U$$

where the derivatives are written in operator-style to the left of the quantity operated upon. This suggests that to get a one-way wave equation out of equation (1), even when velocity is a function of x, all that needs to be done is to take the square root of the operators on both sides of equation (1).

The algorithms used in this thesis all use a continued fraction expansion for the square root of an operator. Alternatively, operator power series or Fourier transforms could also be used to define an operator square root. Thus, the one-way wave equation for upgoing waves in a constant velocity earth is

$$\frac{\partial}{\partial z} U = \left[\frac{1}{v^2}\frac{\partial^2}{\partial t^2} - \frac{\partial^2}{\partial x^2}\right]^{1/2} U \tag{2}$$

Equation (2) can be used to continue a wave downwards in z. Given the pressure wave at depth z, $U(x,z,t)$, the wave at depth $z + \Delta z$ can be found by solving equation (2). Formally, the solution is

$$U(x,z+\Delta z,t) = \exp\left[\Delta z\left[\frac{1}{v^2}\frac{\partial^2}{\partial t^2} - \frac{\partial^2}{\partial x^2}\right]^{1/2}\right] U(x,z,t) \tag{3}$$

The exponential in equation (3) has an operator as its argument, so it must be interpreted in terms of its power series expansion or one of its rational approximations. Later chapters will be devoted to finding adequate rational approximations to equation (3).

Methods for the downward continuation of downgoing wavefields

A relation similar to equation (3) can be used to downward continue a model of the downgoing wave caused by the source, D. This necessitates changes in the initial condition at $z = 0$ and in the differential equation that propagates the wave. The initial condition is altered to model a seismic source, while the differential equation is modified so that it supports downgoing and not upgoing waves. Under certain circumstances, it is desirable to use approximate, analytic solutions to the differential equation.

The surface initial condition for the differential equation for downward continuing the wave caused by the source should be a delta function (or a low-pass filtered delta function) of both lateral position and time. Letting x_s and $f(t)$ denote the lateral position and causal waveform of the shot, respectively, the initial condition takes the form $D(x,0,t) = f(t)\delta(x - x_s)$.

The equation for downward continuation must be altered for a downgoing wave like D. Formally, an equation like equation (3) for this purpose is obtained through a single sign change.

$$D(x,z + \Delta z,t) = \exp\left[- \Delta z\left(\frac{1}{v^2}\frac{\partial^2}{\partial t^2} - \frac{\partial^2}{\partial x^2}\right)^{1/2}\right] D(x,z,t) \qquad (4)$$

Equation (4) can be implemented for the numerical downward continuation of the downgoing wave D.

Getting images from downward continued U's and D's will require stripping off and appropriately scaling that part of U that is time coincident with D. One way to do this is to calculate the frequency domain quotient U/D. Therefore, estimates of $1/D$ will be needed for getting images from downward continued profiles. Unfortunately, there is nothing about the structure of either equation (4)

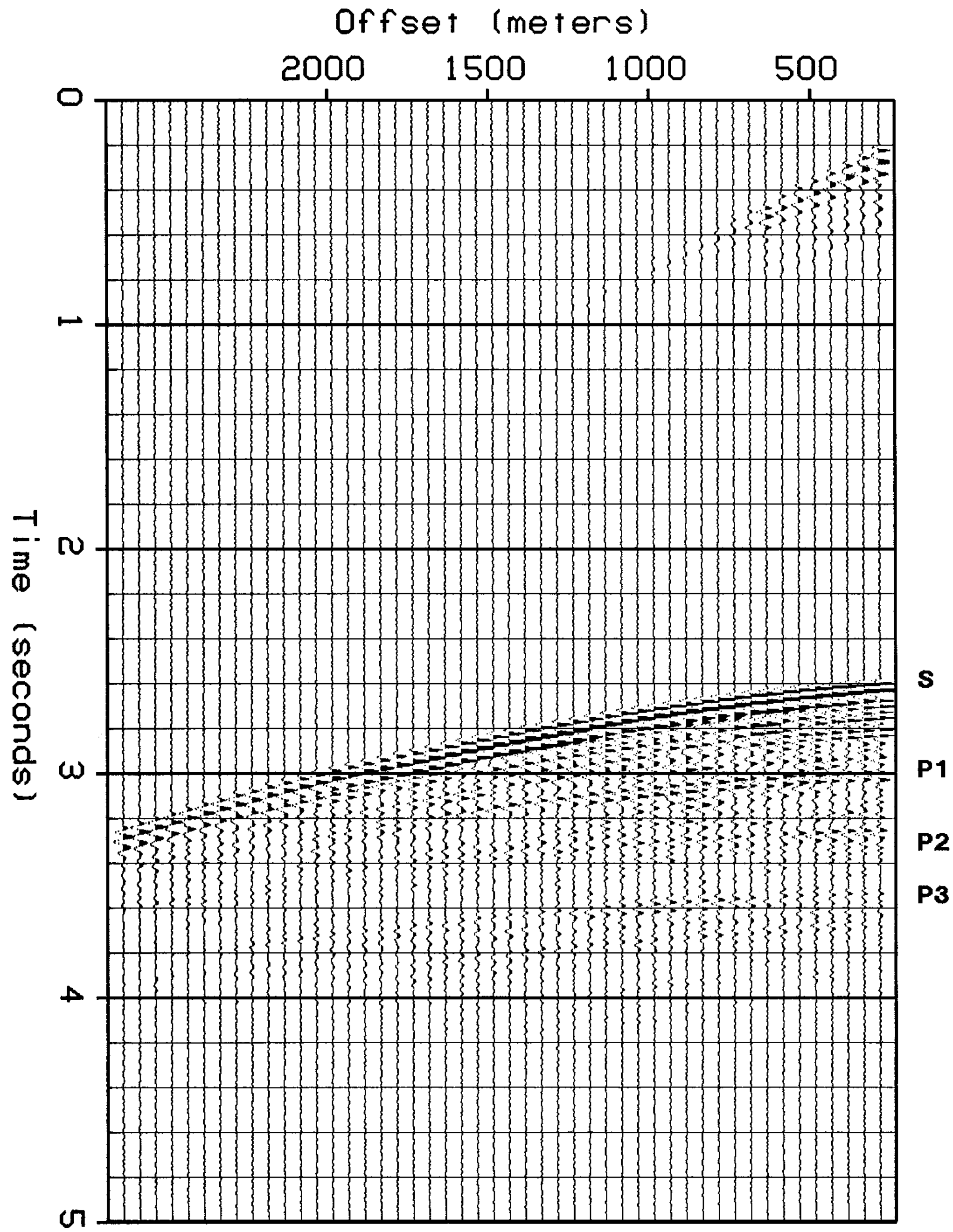

FIGURE 1.1. A marine shot profile. The Cartesian method was used to downward continue the data set in this figure. The data has been trace balanced but is not deconvolved. The near offset, appearing at the far right, is 238 meters distant from the shot. The data is sampled along the geophone axis at a 50 meter rate. The events marked **S** , **P1** , **P2** , and **P3** are primary reflections.

or the initial value of D at $z = 0$ that guarantees $D \neq 0$ everywhere for all frequencies. Spectral zeros can be expected when variable velocity and absorbing side boundaries are used during downward continuation. Therefore, an analytic expression for D, when available, may be preferable to a computationally determined D estimate. Two ways of getting an analytic expression are ray tracing and a rms velocity approximation.

Ray tracing is one way to get the phase information of the downgoing wavefield without really downward continuing the field. In a vertically varying acoustic medium ray tracing from shot position (s,0) to a scatterer position (x,z) is easy, yielding a travel time for the trip along the shot-to-scatterer ray. Let $T(x,z,s,0)$ denote this travel time. Given T, a good approximation to the frequency domain representation of the down-going wave field caused by the shot is

$$\frac{1}{T^{1/2}(x,z,s,0)} e^{i\omega T(x,z,s,0)}$$

The ease with which the ray tracing is done governs the usefulness of this approach. The ray parameter of the ray connecting the shot to the scatterer can be found by iterating according to the scheme

$$p_0 = 0$$

$$p_{k+1} = \frac{x - s}{\int_0^z dz' \frac{V(z')}{\left[1 - p_k^2 V(z')\right]^{1/2}}}$$

that converges as long as the scatterer is not at a position where the ray is either critical or super-critical. In the critical or super-critical cases, the migration output can be set equal to zero. If p is known, T is found by using

$$T = \int_0^z dz' \frac{1}{V(z') \left[1 - p_k^2 V(z')\right]^{1/2}}$$

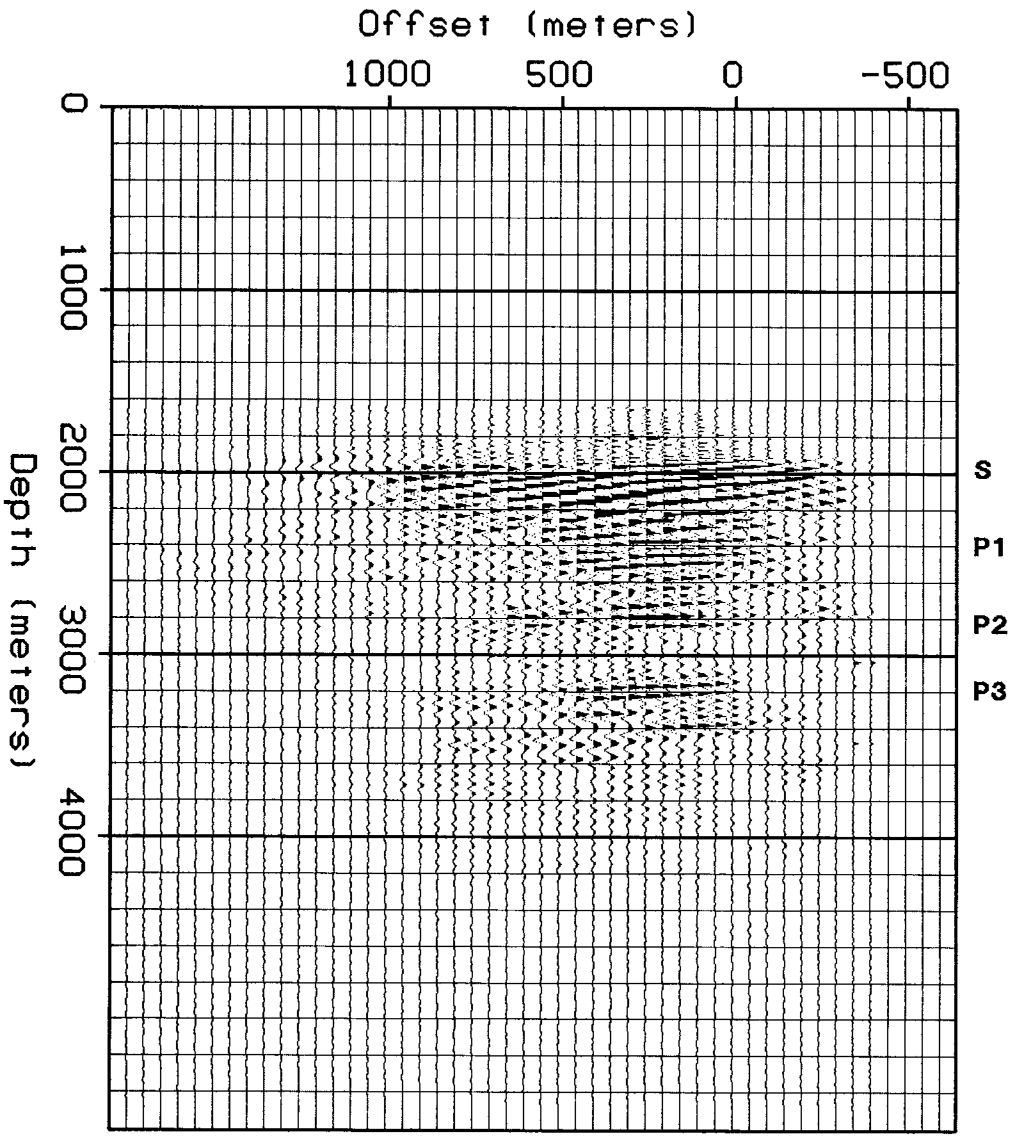

FIGURE 1.2. Cartesian downward continuation and UD^* imaging. The Cartesian method was used to downward continue the data set in figure 1.1. An image was constructed from the downward continued upgoing and downgoing waves using a reflection coefficient estimator of the form ΣUD^*. Zero offset appears some 643.5 meters from the trace at the far right. The geophone spacing on this image is still 50 meters, so the zero offset trace is about 13 traces from the right edge of the plot.

If an analytic representation for the downgoing wave is desired, then T can be approximated by using a root-mean square velocity approximation. This approximation is accurate at near offsets and is incapable of distinguishing between sub-critical and super-critical zones. When the approximation is used to image a downward continued profile, a refraction artifact may dominate the output. The rms velocity approximation for the downgoing wave has the same form as the ray tracing estimate for D, but uses

$$T \approx \frac{1}{V_{rms}} \left[z^2 + (x - s)^2 \right]^{1/2}$$

Imaging by time coincidence of upgoing and downgoing waves

Images of the subsurface can be obtained by frequency domain division of the downward continued upgoing wave by the downward continued downgoing wave. Let $D(s,g,z,t)$ denote the downgoing wave in a profile caused by an impulsive source exploded at time $t = 0$ and lateral position s on the surface of the earth. Let $U(s,g,z,t)$ denote the upgoing wave caused by scattering of $D(s,g,z,t)$. If at depth z there is a planar reflector with reflection coefficient c, then

$$U(s,g,z,t) = \int_0^\infty dt' \left[c(s,g,z)\delta(t - t') \right] D(s,g,z,t') = c(s,g,z)\ D(s,g,z,t') \quad (5)$$

where the reflection coefficient is assumed to have a delta function time dependence. The assumption of delta function time dependence implies that the temporal spectrum of c is flat. An approximation to the reflection coefficient at $t = 0$ can be obtained by adding frequency domain quotients of the form $U(s,g,z\,\omega)/\,D(s,g,z,\omega)$, where $U(s,g,z,\omega)$ and $D(s,g,z,\omega)$ denote the frequency components of the upcoming and downgoing waves of a profile, respectively. Frequency domain division really yields a reflection coefficient $\hat{c}_0$ estimate that may be different from c because of noise contamination. If $N(\omega)$ is the number of discrete frequencies, then one reflection coefficient estimate is

$$\hat{c}_0(s,g,z) = \frac{1}{N(\omega)} \sum_{\omega=1}^{N(\omega)} \frac{U(s,g,z,\omega)}{D(s,g,z,\omega)} \tag{6}$$

If the radiation patterns of the sources are corrected for, and if the migration velocity used in downward continuing U and D was the correct one, then the reflection coefficient will be independent of illumination, so $\hat{c}_0$ will be independent of s. Stacking over s under such conditions would suppress noise and coherent events not modeled by the acoustic wave equation.

The reflection coefficient estimate in equation (6) will not be well behaved if there are zeros in the spectrum of the downgoing wave. Here a noise model must be incorporated in the imaging step. If the noise time series is white and additive, then the convolutional model yields a sequence of increasingly sophisticated and noise sensitive reflection coefficient estimators:

$$\hat{c}_1(s,g,z) = \frac{1}{N(\omega)} \sum_{\omega=1}^{N(\omega)} U(s,g,z,\omega)\, D^*(s,g,z,\omega)$$

$$\hat{c}_2(s,g,z) = \frac{1}{N(\omega)} \sum_{\omega=1}^{N(\omega)} U(s,g,z,\omega)\, \frac{D^*(s,g,z,\omega)}{|D(s,g,z,\omega)|}$$

$$\hat{c}_3(s,g,z) = \frac{1}{N(\omega)} \sum_{\omega=1}^{N(\omega)} U(s,g,z,\omega)\, \frac{D^*(s,g,z,\omega)}{|D(s,g,z,\omega)|^2 + \varepsilon(x^2+z^2)^{1/2}}$$

These estimators differ in their treatment of the amplitude spectrum of D, but preserve the phase information. The estimator $\hat{c}_3$, justified with an argument from linear estimation theory, is the best estimator in the absence of noise. The parameter ε is related to the signal- to-noise ratio. As ε is increased, $\hat{c}_3$ is asymptotically equal to $\hat{c}_1$. In practice, $\hat{c}_3$ is too noise sensitive for the purpose of estimating reflection coefficients using common shot profiles.

Application of the Cartesian method to a marine profile

The most general of the downward continuation algorithms discussed in the preceding sections involved the downward continuation of both upgoing and

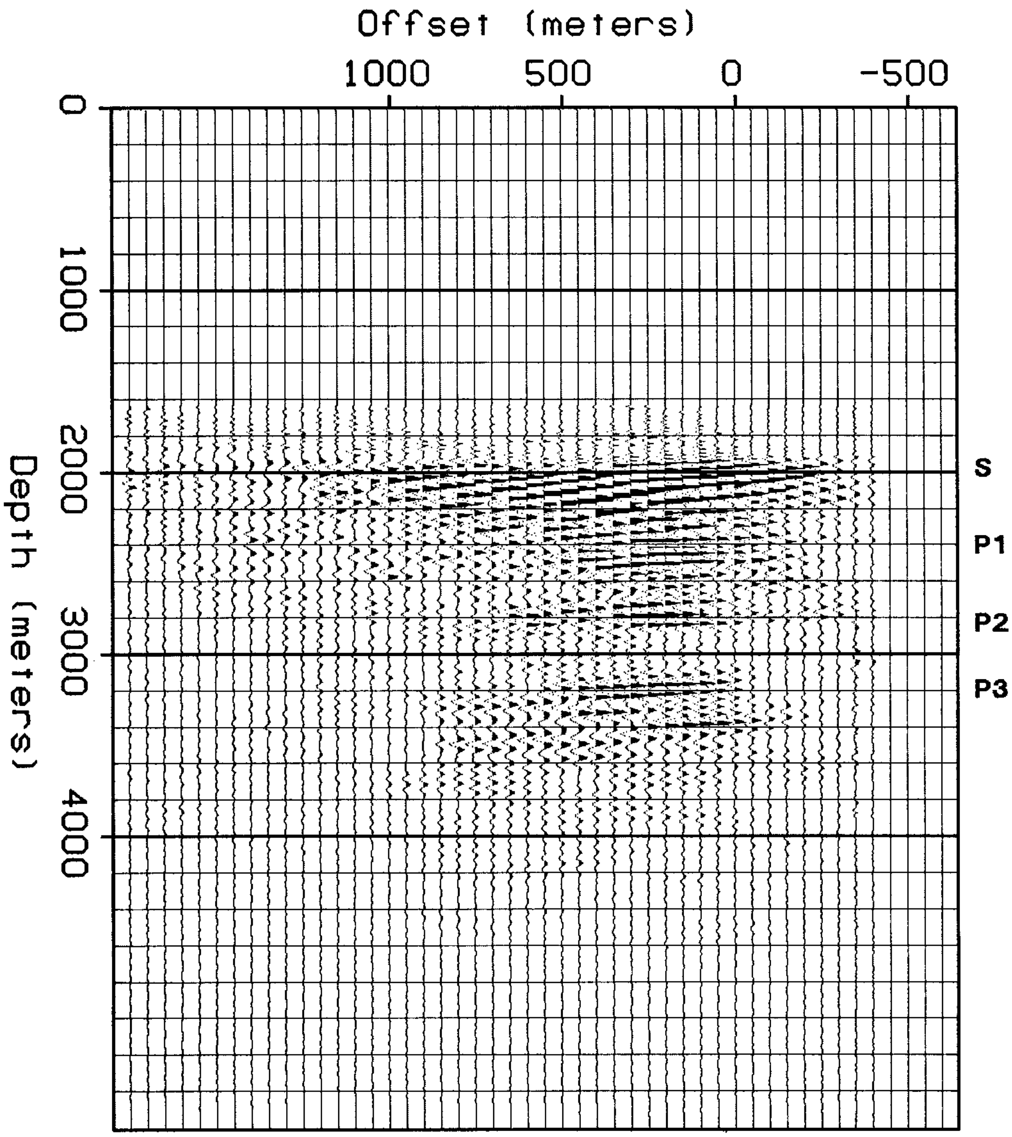

FIGURE 1.3. Cartesian downward continuation and $UD^*/|D|$ imaging. This image was constructed with the same scheme as that in Figure 1.2. This time, however, a reflection coefficient estimator of the form $\Sigma UD^*/|D|$ was used instead of ΣUD^*. The sea-floor reflector at 2000 meters depth is still severely effected by aliasing of the data along the geophone axis. Other important events occur at depths of 2400, 2800, 3200, and 3400 meters.

downgoing waves by computational means. The fully computational Cartesian algorithm is able to extrapolate upgoing and downgoing waves in acoustic media that vary both laterally and vertically. Cartesian algorithms that downward continue the downgoing wave analytically are cheaper but cannot cope with large lateral velocity variations. A computational version of the Cartesian method for downward continuing shot profiles was applied to the marine data set of figure 1.1. The profile has 48 channels spaced 50 meters apart. The near offset distance is 238 meters. The sampling rate along the time axis is 4 milliseconds. Ten seconds of data were recorded, but only the first five seconds were downward continued. Much of this five seconds is devoid of significant acoustic energy, so multiple reflections are absent from the part of the profile under consideration. Finally, a significant lateral velocity variation is present because the depth to the sea floor is increasing with increasing offset.

The results of applying the Cartesian method with reflection coefficient estimators $\hat{c}_1$ and $\hat{c}_2$ appear in figures 1.2 and 1.3, respectively. Implementation of the estimator $\hat{c}_0$ was not even attempted because of its noise sensitivity in regions where D has spectral zeros. The sampling rate along the vertical axes of both plots is 10.57 meters. Because padding applied before the migration, the near offset of the output files is equal to -643.5 meters. Thus, zero-offset occurs about thirteen traces away from the edge of each of the displays.

In implementing the Cartesian method, a constant velocity, frequency domain approach was used to downward continue both upgoing and the downgoing waves through most of the water column. The sampling requirements and dip limitations for the frequency domain algorithm are, of course, far less constraining than those for finite difference operators. Finite difference techniques were used for downward continuing the two waves through the sea floor and sediments.

Apart from a time-variable gain, the plots are remarkably similar. The estimator $\hat{c}_3$ was not implemented satisfactorily because of difficulties associated with choosing a spatially varying ε. Bad choices of ε make $\hat{c}_3$ excessively noise sensitive.